Supporting Information

Cancer cell-targeted cisplatin prodrug delivery *in vivo via* metabolic labeling and bioorthogonal click reaction

Xun Liu,[a,¶] Fan Wu,[a,¶] Kaimin Cai,[b] Ziyin Zhao,[a] Zhimin Zhang,[a] Yongbing Chen,[c] Yong Liu,[a] Jianjun Cheng,[b,*] and Lichen Yin [a,*]

[a] Institute of Functional Nano and Soft Materials (FUNSOM), Jiangsu Key Laboratory of Carbon-Based Functional Materials and Devices, Collaborative Innovation Center of Suzhou Nano Science & Technology, Soochow University, Suzhou 215123, China.

[b] Department of Materials Science and Engineering, University of Illinois at Urbana-Champaign, Urbana, Illinois 61801, United States.

[c] Department of Thoracic Surgery, the Second Affiliated Hospital of Soochow University, Suzhou 215004, China

[¶] These authors contributed equally.

Correspondence and requests for materials should be addressed to J.C. (email: jianjunc@illinois.edu) or to L.Y. (email: lcyin@suda.edu.cn).

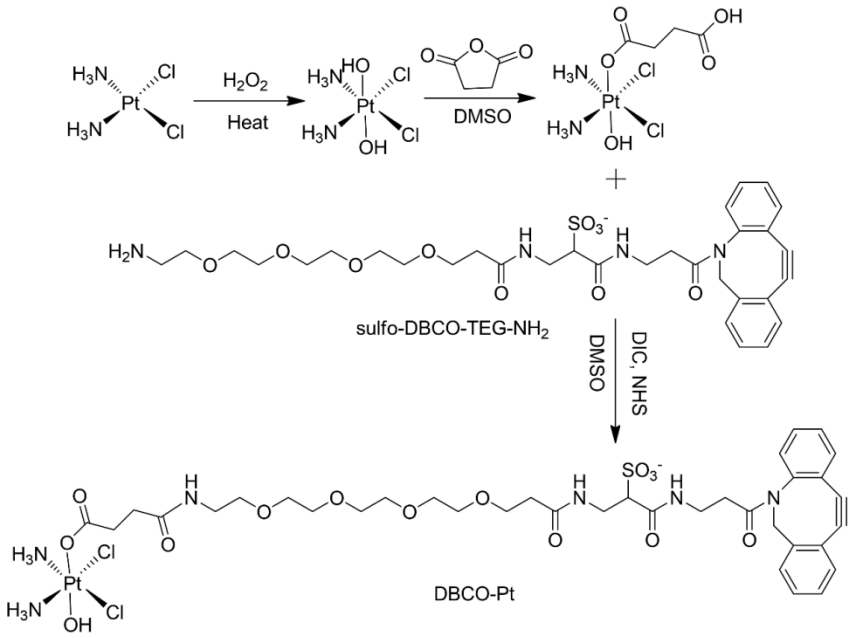

Scheme S1. Synthetic route of DBCO-Pt.

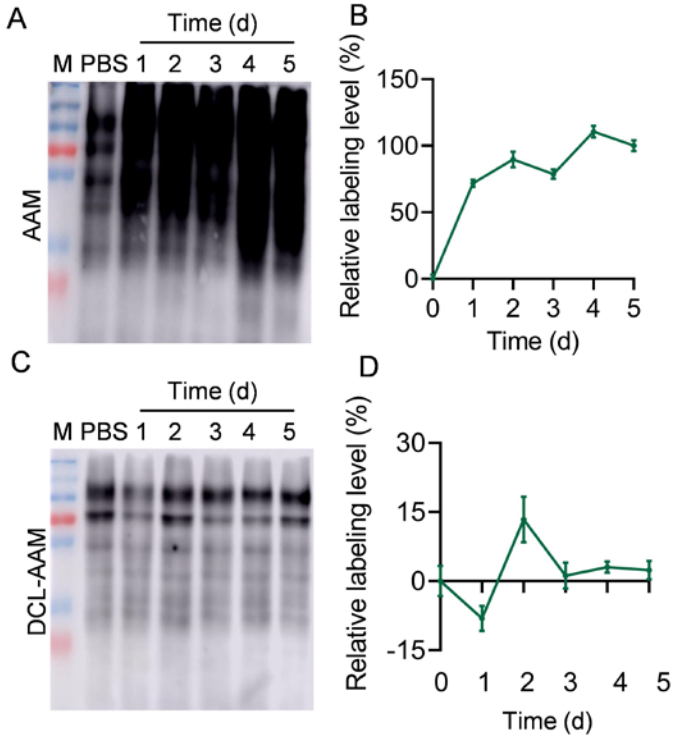

Figure S1. *In vitro* labeling kinetics of AAM (A-B) and DCL-AAM (C-D) in RAW 264.7 cells. Western blot analyses showing the metabolic expression of cell-surface azido groups in RAW 264.7 cells after incubation with AAM (A) or DCL-AAM (C). Relative labeling level of AAM (B) and DCL-AAM (D) calculated from Western blot analyses in (A) and (C), respectively, using the ImageJ software (n = 3). M represents marker.

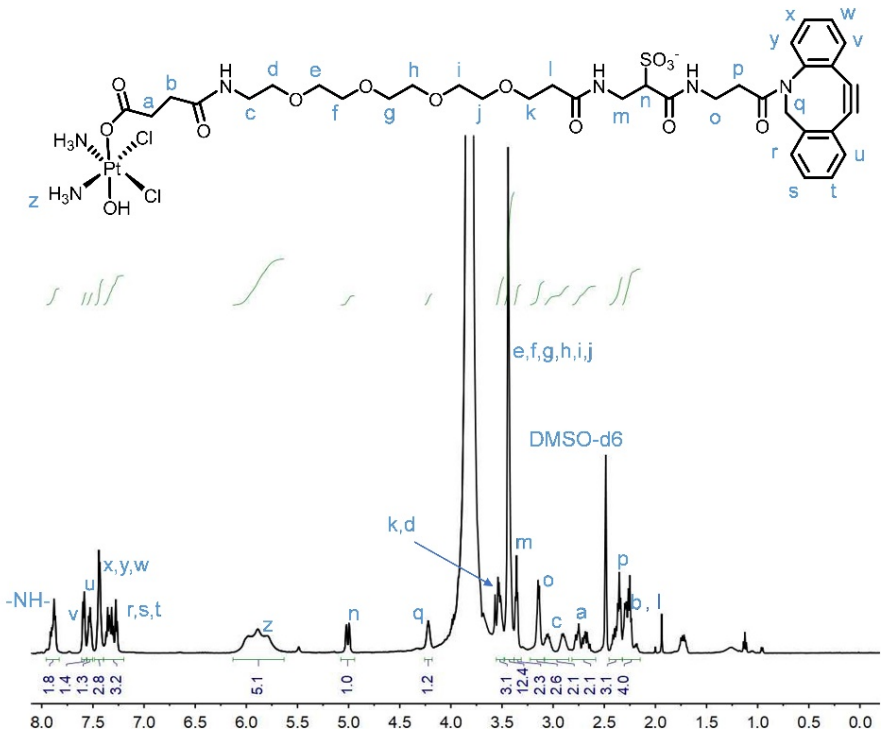

Figure S2. ^{1}H NMR spectrum of DBCO-Pt in DMSO-d_6.

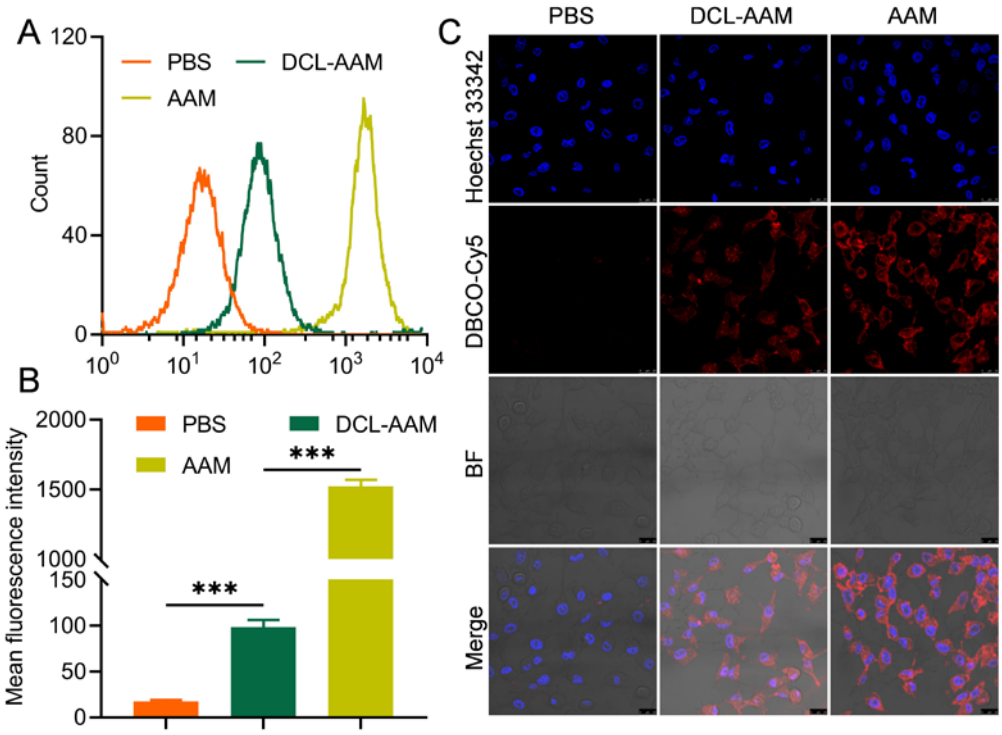

Figure S3. (A) Flow cytometry analyses showing the cellular uptake of DBCO-Cy5 in SKOV3 cells after incubation with DCL-AAM (50 μM) or AAM (50 μM) for 48 h followed by incubation with DBCO-Cy5 (50 μM) for another 1 h. (B) Mean fluorescence intensity per cell as calculated from flow cytometry analyses in (A) (n = 3). (C) CLSM images of SKOV3 cells following the same treatment in (A). Scale bar = 25 μm.

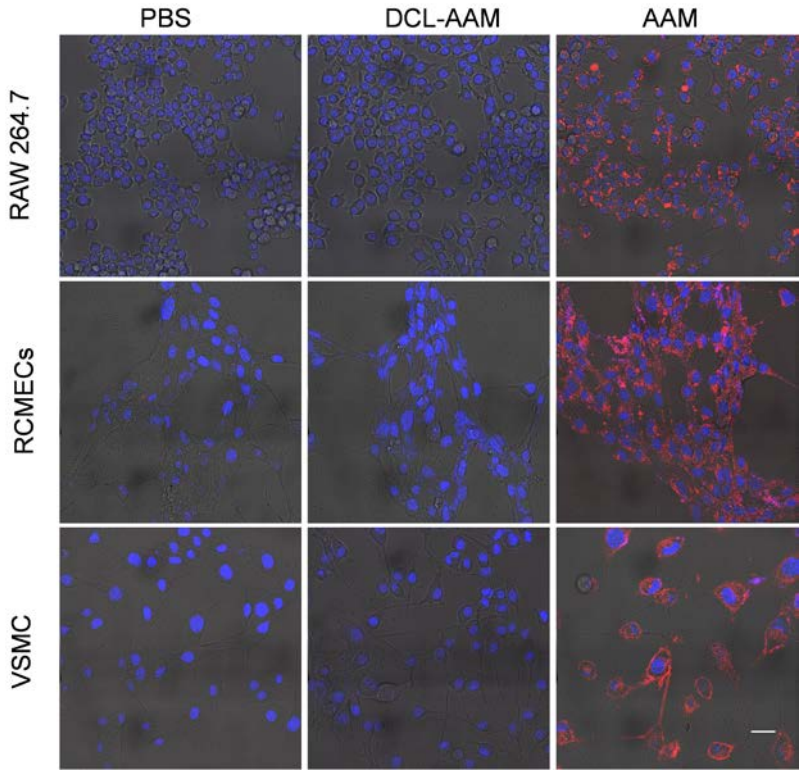

Figure S4. CLSM images of RAW 264.7, RCMECs, and VSMC cells after incubation with PBS, DCL-AAM (50 μM), or AAM (50 μM) for 48 h and labeling with DBCO-Cy5 (50 μM) for 1 h (scale bar = 25 μm).

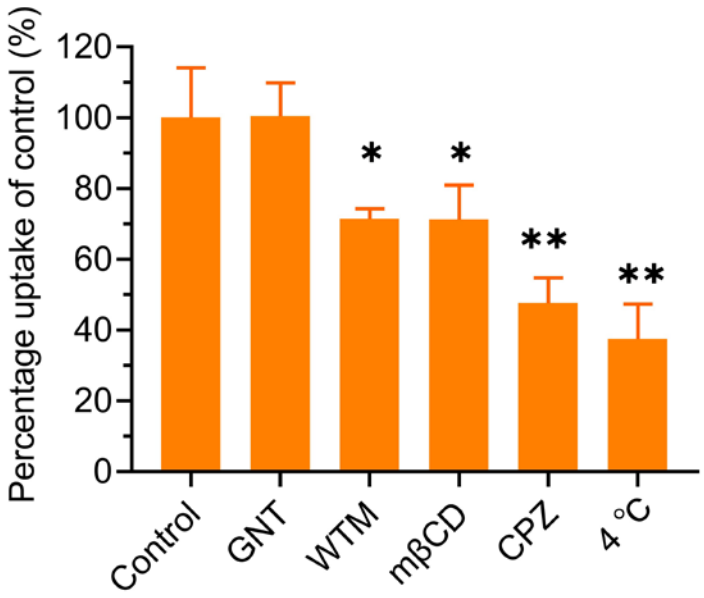

Figure S5. Cellular uptake level of DBCO-Cy5 in SKOV3 cells pre-treated with DCL-AAM (50 μM) for 48 h. DBCO-Cy5 (50 μM) was incubated with cells for 1 h at 4 °C or in the presence of chlorpromazine (CPZ, 10 μg/mL), genistein (GNT, 100 μg/mL), methyl-β-cyclodextrin (m β CD, 50 μM), or wortmannin (WTM, 50 nM) at 37 °C (n = 3).

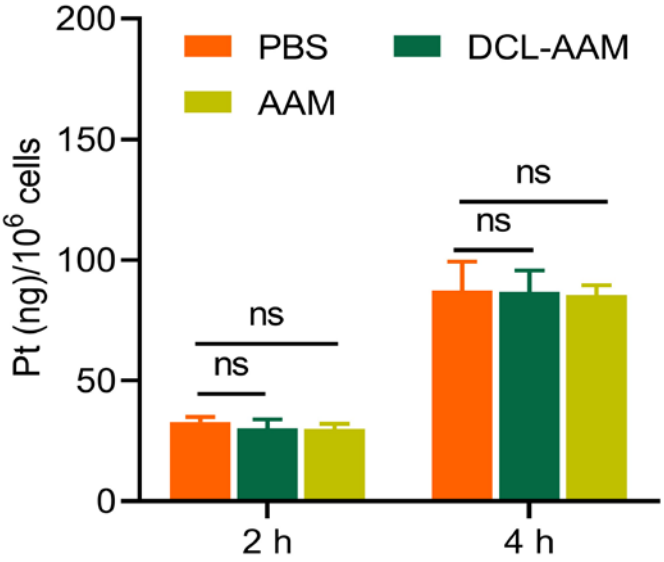

Figure S6. Amount of the internalized Pt in SKOV3 cells after pre-treatment with PBS, DCL-AAM (50 μM), or AAM (50 μM) for 48 h followed by incubation with CDDP (50 μM) for 2 or 4 h (n = 3).

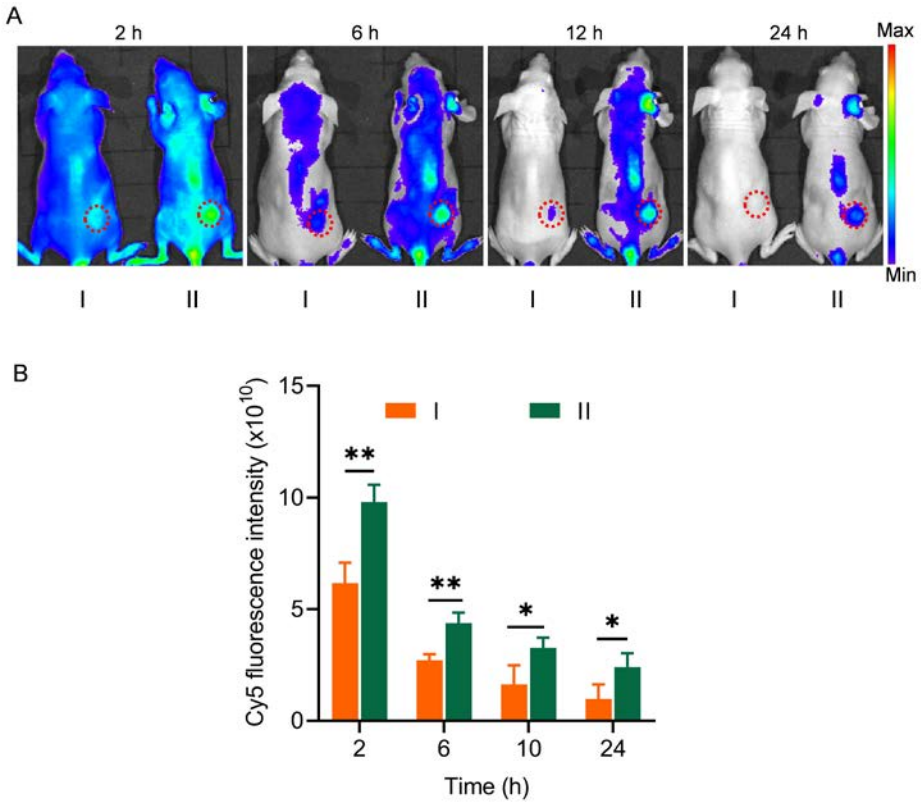

Figure S7. (A) Representative fluorescent images of SKOV3 tumor-bearing mice at various time intervals post *i.v.* injection of DBCO-Cy5 (5 mg/kg). PBS (I) or DCL-AAM (II, 60 mg/kg) was i.v. injected once daily for three consecutive days before *i.v.* injection of DBCO-Cy5. (B) Quantitative analysis of Cy5 fluorescence intensity at the tumor sites as indicated by the dashed circles in (A) (n = 3).

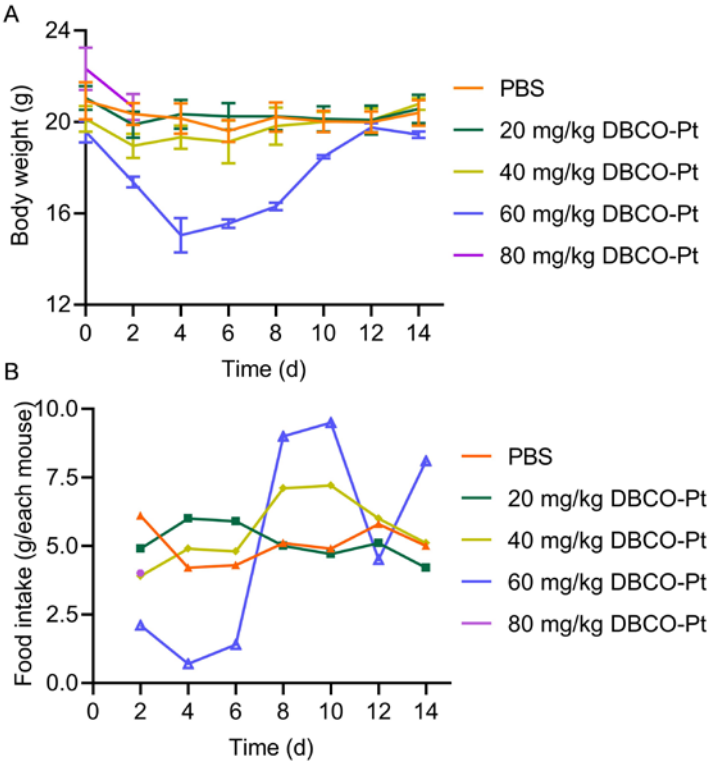

Figure S8. Variations of body weight (A) and food intake (B) of mice within the 14-d observation periodafter being *i.v.* injected with PBS or DBCO-Pt at various doses (n = 6).

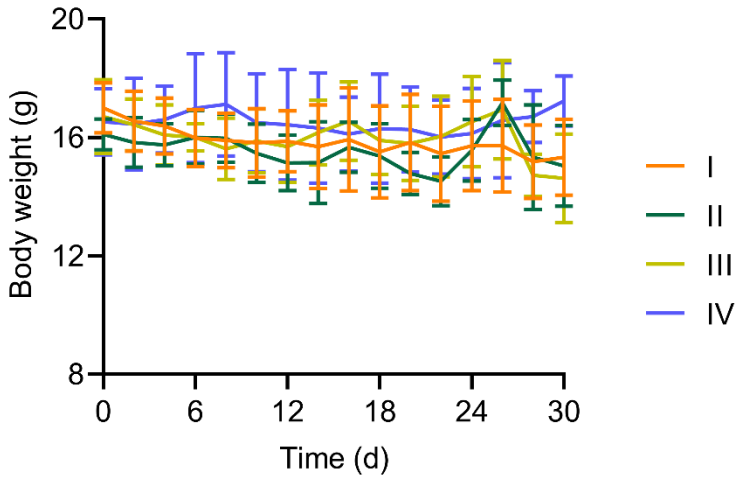

Figure S9. Body weight change of SKOV3 tumor-bearing mice in the *in vivo* efficacy study (n = 13). I: PBS; II: DCL-AAM (60 mg/kg) + Pt (5 mg/kg); III: PBS + DBCO-Pt (20 mg/kg); IV: DCL-AAM (60 mg/kg) + DBCO-Pt (20 mg/kg).

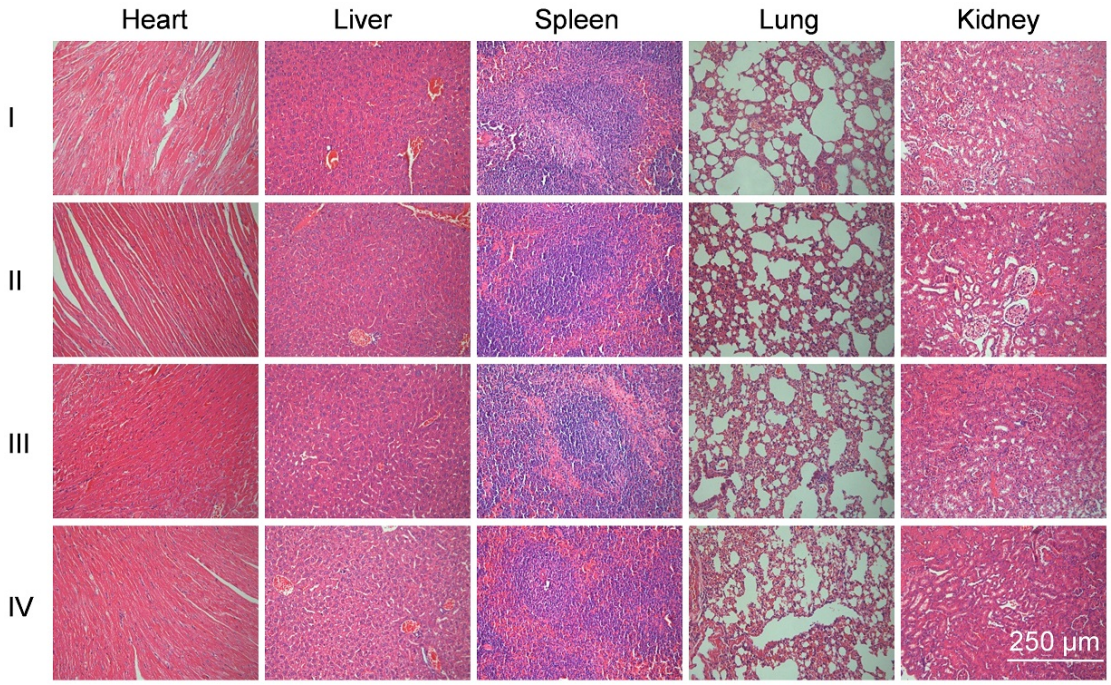

Figure S10. Histological analysis of the H&E-stained major organ sections from the SKOV3 tumor-bearing mice collected on day 30 in the *in vivo* efficacy study. Scale bar = 250 μm. I: PBS; II: DCL-AAM (60 mg/kg) + Pt (5 mg/kg); III: PBS + DBCO-Pt (20 mg/kg); IV: DCL-AAM (60 mg/kg) + DBCO-Pt (20 mg/kg).

Table S1. IC_{50} values of Pt in various treatments against SKOV3 cells.

Formula	IC_{50} (μM)
DBCO-Pt	607.4
DCL-AAM + DBCO-Pt	449.2
AAM + DBCO-Pt	266.8
CDDP	160.9
DCL-AAM + CDDP	165.8
AAM + CDDP	149.2